

·学术前沿:肠道菌群与屏障功能专题·

## 肠道菌群和中晚期肝癌 TACE 联合靶向免疫治疗预后相关性

刘航, 朱博文, 范文哲, 李家平, 吴艳琴  
(中山大学附属第一医院肿瘤介入科, 广东广州 510080)

**摘要:**【目的】探讨中晚期肝细胞癌(HCC)患者经动脉化疗栓塞(TACE)联合靶向免疫治疗后肠道菌群组的特征及与预后的关联。【方法】本研究回顾性收集2025年2月至2025年7月就诊中山大学附属第一医院并接受过TACE联合靶向免疫治疗的中晚期肝细胞癌患者临床资料,采集患者本次入院治疗前的粪便样本。根据无进展生存期(PFS)是否达到6个月,分为预后好组与预后差组;按照修正后实体瘤疗效评价标准(mRECIST)评估首次TACE术后是否缓解,分为应答组与无应答组。采用宏基因组测序技术对粪便菌群测序,通过生信分析判断两组肠道细菌与真菌群落的多样性、组成差异,筛选预后相关的特征性菌群。【结果】共计61例患者符合标准。 $\alpha$ 多样性及 $\beta$ 多样性分析,两种分组方式组间细菌、真菌多样性均无统计学差异( $P>0.05$ )。在细菌层面,约氏乳杆菌(预后分组 $P=0.048$ ,应答分组 $P=0.043$ )、齿双歧杆菌(预后分组 $P=0.004$ ,应答分组 $P=0.030$ )和艰难梭菌(预后分组 $P=0.017$ ,应答分组 $P=0.016$ )在预后好组和应答组中均显著富集。真菌层面,十齿隐球菌( $P=0.045$ )、条锈菌( $P=0.002$ )、嗜树克沃尼埃拉菌( $P=0.015$ )在预后好组中富集;叶斑病菌( $P=0.037$ )在应答组中富集;毒蝇钩霉菌( $P=0.024$ )在无应答组中富集。按照两种分组的共同差异菌丰度分别进行生存分析,结果显示齿双歧杆菌的丰度与患者预后存在显著关联。【结论】肠道菌群的差异同中晚期肝癌TACE联合靶向免疫治疗的预后相关,齿双歧杆菌可能作为评估联合治疗疗效的潜在预测指标或影响其疗效的潜在干预途径。肠道真菌群的差异可能与中晚期肝癌TACE联合靶向免疫治疗的预后相关。

**关键词:**肝细胞癌;肠道菌群;经动脉化疗栓塞;免疫治疗;靶向治疗

中图分类号:R735.7

文献标志码:A

文章编号:1672-3554(2026)03-0397-12

DOI: 10.11714/jysu.med.YX20260040

## Association Analysis Between Gut Microbiota and Prognosis in Patients with Intermediate-to-advanced Hepatocellular Carcinoma Treated with TACE Combined with Targeted Therapy and Immunotherapy

LIU Hang, ZHU Bowen, FAN Wenzhe, LI Jiaping, WU Yanqin

(Department of Interventional Oncology, The First Affiliated Hospital, Sun Yat-sen University, Guangzhou 510080, China)

Correspondence to: WU Yanqin; Email: wuyq73@mail.sysu.edu.cn

**Abstract:**【Objective】To characterize the features of the gut microbiome and its association with clinical prognosis in patients with intermediate and advanced hepatocellular carcinoma (HCC) treated with transcatheter arterial chemoembolization (TACE) combined with targeted therapy and immunotherapy.【Methods】This retrospective study enrolled patients with intermediate and advanced HCC who received TACE combined with targeted therapy and immunotherapy at the First Affiliated Hospital of Sun Yat-sen University from February 2025 to July 2025. Baseline clinical data and fecal samples were collected from all enrolled patients before the index hospitalization and treatment. Patients were stratified using two independent criteria: ① a good-prognosis group and a poor-prognosis group, based on

收稿日期:2026-03-14

录用日期:2026-04-23

基金项目:广东省自然科学基金(2026A1515012039)

作者简介:刘航,第一作者,研究方向:肝细胞癌的微创治疗,E-mail: liuh523@mail2.sysu.edu.cn;吴艳琴,通信作者,副主任医师,  
E-mail: wuyq73@mail.sysu.edu.cn

whether progression-free survival (PFS) reached 6 months; ② a response group and a non-response group, based on tumor response to the first TACE assessed by the modified Response Evaluation Criteria in Solid Tumors (mRECIST). Metagenomic sequencing was performed on fecal samples. Bioinformatic analysis was conducted to evaluate the diversity and compositional differences of intestinal bacterial and fungal communities between groups in each stratification, and to screen for prognosis-associated characteristic microbial taxa. 【Results】 A total of 61 patients met the inclusion criteria. Analysis of  $\alpha$ -diversity and  $\beta$ -diversity showed no statistically significant differences in bacterial and fungal diversity between groups under either stratification strategy ( $P > 0.05$ ). At the bacterial level, *Lactobacillus johnsonii* (prognosis stratification:  $P=0.048$ ; response stratification:  $P=0.043$ ), *Bifidobacterium dentium* (prognosis stratification:  $P=0.004$ ; response stratification:  $P=0.030$ ) and *Clostridioides difficile* (prognosis stratification:  $P=0.017$ ; response stratification:  $P=0.016$ ) were significantly enriched in both the good prognosis group and the response group. At the fungal level, *Cryptococcus decaguttatus* ( $P=0.045$ ), *Puccinia striiformis* ( $P=0.002$ ), and *Kwoniella quercicola* ( $P=0.015$ ) were enriched in the good-prognosis group; *Kwoniella bestiolae* ( $P=0.037$ ) was enriched in the response group; and *Akanthomyces muscarius* ( $P=0.024$ ) was enriched in the non-response group. Survival analysis based on the common differential bacterial abundance in both groupings showed a significant correlation between the abundance of *Bifidobacterium dentium* and patient prognosis. 【Conclusion】 Differences in the gut microbiota are associated with the prognosis of patients with intermediate and advanced HCC treated with TACE combined with targeted therapy and immunotherapy. *Bifidobacterium dentium* may serve as a potential predictive biomarker for the efficacy of this combination regimen, and represents a potential intervention target to modulate treatment response. Differences in gut fungal communities are also potentially associated with the prognosis of intermediate and advanced HCC patients receiving TACE combined with targeted therapy and immunotherapy.

**Key words:** hepatocellular carcinoma; gut microbiota; transarterial chemoembolization; immunotherapy; targeted therapy

[J SUN Yat-sen Univ (Med Sci), 2026, 47(3): 397-408]

肝细胞癌 (hepatocellular carcinoma, HCC) 是全球癌症相关死亡的主要原因之一, 多数患者确诊时已属中晚期, 预后不佳<sup>[1-2]</sup>。经导管动脉化疗栓塞 (transarterial chemoembolization, TACE) 联合靶向及免疫治疗已成为中晚期 HCC 的标准治疗模式, 可显著改善部分患者的生存<sup>[3-5]</sup>。然而, 该联合疗法的疗效存在显著的个体异质性, 其预测与预后评估仍是临床面临的重大挑战<sup>[6]</sup>。近年来, “肠-肝轴”在 HCC 发生发展中的作用备受关注。肠道菌群失调可通过破坏肠屏障、促进细菌/内毒素易位、改变菌群代谢谱以及调节宿主免疫, 持续加剧肝脏炎症与免疫抑制, 从而驱动 HCC 的演进<sup>[7-10]</sup>。与此同时, 肠道菌群组作为关键的宿主免疫调节器, 已被证实能显著影响多种癌症对免疫检查点抑制剂的治疗反应<sup>[11-13]</sup>。值得注意的是, TACE 作为局部治疗手段, 其本身可能诱发缺血-再灌注损伤与全身炎症, 进而扰动肠道菌群的稳定性<sup>[14]</sup>。有研究发现 HCC 患者在接受 TACE 后, 肠道菌群多样性显著降低, 且特定菌属 (如拟杆菌属、粪杆菌属) 的丰度变化以

及某些代谢产物如吲哚-3-乳酸的水平与术后肝功能恢复情况及炎症指标水平相关<sup>[14-16]</sup>。另有研究提示, 富含某些产短链脂肪酸菌 (如罗斯氏菌属) 的肠道生态, 与更好的 TACE 后肿瘤反应性相关<sup>[17]</sup>。在 HCC 的治疗领域, 除 TACE 外, 肠道菌群在免疫治疗中的作用亦积累了丰富的临床证据。基线肠道菌群的多样性以及富含某些特定的“有益菌”, 对于 HCC 免疫治疗应答及预后均有预测意义<sup>[13, 18-20]</sup>。动物实验表明, 清除肠道菌群会降低索拉非尼的抗肿瘤效果, 而补充特定益生菌可恢复其疗效<sup>[21]</sup>。然而, 肠道菌群与 TACE 联合靶向免疫治疗这一综合模式之间的相互作用与临床关联, 目前尚缺乏系统的研究阐明。本研究更加全面地分析该治疗模式下患者肠道菌群组的构成特征, 并探究其与临床结局的关联, 以期寻找新的疗效预测生物标志物和干预靶点。本研究旨在为提升中晚期 HCC 患者的整体生存获益贡献新的科学视角与策略。

## 1 材料与方

### 1.1 研究对象

本研究为一项回顾性研究,纳入了2025年2月至2025年7月期间在中山大学附属第一医院就诊并接受过TACE联合靶免治疗的61例中晚期HCC患者。主要纳入标准包括:①依据《原发性肝癌诊疗指南(2024年版)》诊断为HCC,按照中国肝癌的分期方案(China Liver Cancer Staging, CNLC)分期为Ⅱa~Ⅲb期<sup>[22]</sup>。②肝功能Child-Pugh分级A或B级;③美国东部肿瘤协作组体力状况评分为0~2分;④至少存在1个可通过修正后实体瘤疗效评价标准(modified response evaluation criteria in solid tumors, mRECIST)评估的可测量病灶<sup>[23]</sup>;⑤接受过TACE联合靶免治疗且在治疗周期前可采集到新鲜晨便标本。排除标准为:①粪便采集前1个月内使用过抗生素、益生菌或益生元;②未控制的代谢性疾病或活动性感染;③有炎症性肠病或肠易激综合征病史;④临床资料不全。本研究方案经中山大学附属第一医院伦理委员会批准(伦理号:[2024]208),并遵循1964年赫尔辛基宣言(2008年修订版)的伦理准则进行,所有入组患者均签署了知情同意书。

### 1.2 标本收集及测序

收集患者入院24 h内的新鲜粪便作为样本,收集后2 h内送-80 °C冰箱保存。使用DNA提取试剂盒(天根生化科技有限公司,北京)分离DNA。文库构建以每个样本0.2 μg DNA为起始投入量。基因组DNA经Covaris LE220R-plus超声破碎仪(Covaris,美国)打断至350 bp左右,随后对DNA片段进行末端修复和3'端加A处理,连接Illumina测序接头后经PCR扩增。扩增产物用AMPure XP磁珠(Beckman Coulter,美国)纯化,Agilent 5400系统(AATI)检测文库片段大小,合格文库以qPCR方式定量(有效浓度1.5 nmol/L)。各样本文库按有效浓度与目标下机数据量等比混合,最终在Illumina测序平台以PE150策略完成测序(诺禾致源生物科技有限公司,北京)。

### 1.3 治疗方案与评估分组

所有患者接受标准TACE联合靶免治疗。①TACE:采用Seldinger技术穿刺股动脉,超选择至肿瘤供血动脉,注入碘化油(江苏恒瑞医药股份有限

公司,中国)载法码新(无锡辉瑞制药有限公司,中国)混悬液,血流速度减慢后继续注入100~300 μm Callisphere(江苏恒瑞医药股份有限公司,中国)载法码新40 mg混悬液若干进行栓塞。TACE治疗次数为1~3次,根据TACE术后1个月的影像学评估决定是否需要后续TACE。②免疫治疗:使用PD-1抗体药物(信迪利单抗/卡瑞利珠单抗/替雷利珠单抗,200 mg/次,每3周1次)。③靶向治疗:联合贝伐珠单抗(7.5或15 mg/kg,每3周1次)。所有患者均采用统一的治疗顺序:先行TACE治疗,在TACE术后1个月开始联合静脉输注靶向药物及免疫检查点抑制剂。靶免治疗方案如前述,虽具体药物(信迪利单抗/卡瑞利珠单抗/替雷利珠单抗)存在选择,但均为同类作用机制的药物,且给药方案标准化。随访期间,所有患者均未接受除上述方案外的其他抗肿瘤治疗。

通过查看影像学资料评估肿瘤反应,并依据mRECIST标准判定为完全缓解(complete response, CR)、部分缓解(partial remission, PR)、疾病稳定(stable disease, SD)或疾病进展(progressive disease, PD)。基于临床资料评估结果,将无进展生存期(progression-free survival, PFS)达到6个月及以上分为预后好组(A组),将PFS少于6个月分为预后差组(B组)。依据首次TACE后评估影像学缓解(即CR+PR)分为应答组(A组),将评估未达影像学缓解(即SD+PD)分为无应答组(B组)。主要终点为PFS,次要终点为总体生存期(overall survival, OS)。本研究随访截止2025年12月31日。

### 1.4 生物信息学分析

本研究基于宏基因组测序所得的物种丰度矩阵与临床信息,在R语言环境中进行下游统计分析。所有分析前,均通过样本名对菌群数据与临床数据进行严格对齐。

1.4.1 数据处理 原始测序数据经质量控制和修剪后,使用专业流程进行物种注释,生成细菌与真菌的物种丰度表,作为后续所有分析的输入矩阵。

1.4.2 菌群多样性分析 为评估菌群群落特征,进行了以下分析:①α多样性分析:计算Chao1、香农指数(Shannon)等指数,以反映样本内物种的丰富度和均匀度;组间总体差异采用Kruskal-Wallis检验,采用bonferroni法作两两比较。②β多样性分析:计算Bray-Curtis等距离矩阵,并通过主坐标分析(principal coordinates analysis, PCoA)进行可视

化,以展示样本间群落结构的差异;组间群落结构差异采用 PERMANOVA,组内离散度采用 betadisper 并进行 Tukey 事后比较。③群落结构分析:基于属/种水平相对丰度表,在每个分组内按平均丰度筛选排名靠前单元(属的前10、种前20),绘制分组箱线图并拼图展示。

1.4.3 差异物种鉴定 为识别与患者预后或治疗应答相关的关键菌群标志物,采用多方法联合策略。首先,分别运用线性判别分析(Linear discriminant analysis effect size, LEfSe)分析等方法筛选在不同临床分组间丰度存在统计学差异的细菌与真菌物种。随后,整合各方法结果,并通过 LEfSe 的线性判别分析效应值(linear discriminant analysis effect size, LDA)展示各组重要性排名前10的差异物种。差异显著性阈值设定为 LDA 评分 $>2.0$ 。

1.4.4 差异菌生存分析 为评估关键差异物种的预后预测价值,按物种丰度中位数分组,分别在 OS/PFS 终点进行 Kaplan-Meier 分析(survfit)和 log-rank 检验(survdiff)。为评估菌群的预后预测价值,分别使用菌群、临床分期(CNLC)、肿瘤负荷(up-to-seven)及血清甲胎蛋白(Alpha-fetoprotein, AFP)特征构建随机森林分类模型,用于比较不同模型对分组状态的区分能力。模型采用分层重复5折交叉验证,在每个训练折内部使用 Wilcoxon 检验进行特征预筛选,避免全样本先筛选带来的信息泄露。随机森林使用概率分类模式训练,输出交叉验证预测结果、ROC 曲线、AUC 及其95%置信区间。

## 1.5 统计学分析

采用 SPSS 25.0 软件和 R 4.3.3 版本进行统计分析。计量资料首先使用 Shapiro-Wilk 检验进行正态性检验,使用 Levene 检验进行方差齐性检验。符合正态分布的计量资料以均数 $\pm$ 标准差表示,组间比较采用  $t$  检验;非正态分布资料以中位数(四分位间距)表示,组间比较采用 Mann-Whitney  $U$  检验。通过受试者工作特征曲线评估关键菌群标志物的诊断效能。菌群丰度与临床变量间的相关性采用斯皮尔曼等级相关分析。以双侧  $P < 0.05$  为差异有统计学意义。

## 2 结果

### 2.1 研究对象的临床基线特征

初始纳入中晚期 HCC 患者 80 例,经纳排标准

筛选,剔除 16 例(不符合纳入标准 7 例,符合排除标准 9 例);后续随访中 3 例患者失访,最终 61 例患者纳入研究。根据预后情况分为预后好组 38 例和预后差组 23 例;根据首次 TACE 术后是否影像学缓解分为应答组 45 例和无应答组 16 例(附图)。在不同分组方式下,各组间的年龄、性别、临床分期、肿瘤数量及肿瘤最大直径等基线指标比较,差异均无统计学意义( $P > 0.05$ ;附表),表明研究对象的基线资料均衡可比。



附表和附图  
Appendix table  
and figure

### 2.2 宏基因组测序

经宏基因组测序分析,列出属水平和种水平上样本不同分组中相对丰度排名前10的细菌组成:预后好组、预后差组、应答组和无应答组均以拟杆菌属(*Bacteroides*)为主要菌属;普通拟杆菌(*Phocaeicola vulgatus*)、普拉梭菌(*Faecalibacterium prausnitzii*)在各组种丰度均排名靠前(图1)。

### 2.3 多样性分析

对按照预后分组和按照首次 TACE 后有无缓解分组进行组间  $\alpha$  及  $\beta$  多样性分析,两种分组方式的组间细菌、真菌多样性差异均无统计学意义( $P > 0.05$ ;图2)。

### 2.4 差异细菌分析

通过线性判别分析列出组间差异排名前10的菌种:多枝托氏菌(*Thomasclavelia ramosa*;  $P=0.029$ )、卢蒂布劳特氏菌(*Blautia luti*;  $P=0.033$ )、约氏乳杆菌(*Lactobacillus johnsonii*, *L. johnsonii*;  $P=0.048$ )、无害梭菌(*Clostridium innocuum*;  $P=0.011$ )、汉森布劳特氏菌(*Blautia hansenii*;  $P=0.005$ )、齿双歧杆菌(*Bifidobacterium dentium*, *B. dentium*;  $P=0.004$ )、艰难梭菌(*Clostridioides difficile*, *C. difficile*;  $P=0.017$ )、小布劳特氏菌(*Blautia parvula*;  $P=0.014$ )、梭菌属 10cd\* (*Clostridium* sp. 10cd\*;  $P=0.013$ )、盲肠肠球菌(*Enterococcus cecorum*;  $P=0.045$ )在预后好组显著富集;唾液链球菌(*Streptococcus salivarius*;  $P=0.008$ )、唾液乳杆菌(*Ligilactobacillus salivarius*;  $P=0.003$ )、拟杆菌属 KFT8(*Bacteroides* sp. KFT8;  $P=0.047$ )、*L. johnsonii* ( $P=0.043$ )、发酵乳杆菌(*Limosilactobacillus fermentum*;  $P=0.032$ )、卷曲乳杆菌(*Lactobacillus crispatus*;  $P=0.008$ )、*B. dentium* ( $P=0.030$ )、嗜热链球菌(*Streptococcus thermophilus*;  $P=0.032$ )、嗜淀粉乳

杆菌(*Lactobacillus amylovorus*;  $P=0.038$ )、*C. difficile* ( $P=0.016$ )在应答组显著富集;真菌层面,条锈菌(*Puccinia striiformis*, *P. striiformis*;  $P=0.002$ )、嗜树克沃尼埃拉菌(*Kwoniella dendrophila*, *K. dendrophila*;  $P=0.015$ )、十齿隐球菌(*Cryptococcus decagattii*, *C. decagattii*;  $P=0.045$ )在预后好组中富集;叶斑病菌(*Kwoniella bestiolae*, *K. bestiolae*)在应答组中富集( $P=0.037$ );毒蝇钩霉菌(*Akanthomyces muscarius*)在无应答组中富集( $P=0.024$ ;图3)。其中*L. johnsonii*、*B. dentium*、*C. difficile*在预后好组和应答组中均显著富集( $P<0.05$ )。

### 2.5 差异菌的生存分析

将在两种分组方式的A组(预后好组/应答组)中均显著富集的菌种按照丰度分组进行生存分析:按*B. dentium*丰度分组以PFS为终点的生存分析,其组间生存率差异具有统计学意义( $P=0.049$ );其余差异菌丰度分组的组间生存率差异无统计学意义( $P>0.05$ ;图4)。

在菌群、临床分期、肿瘤负荷、AFP特征构建的预后预测模型中,菌群模型的预测效能最高( $AUC = 0.769$ ;图5A-D)。基于随机森林模型的特征重要性分析显示,*B. dentium*的相对丰度是菌群模型预后分类中最重要预测因子(图5E)。

### 2.6 病历展示

按照*B. dentium*丰度分组,选取不同组中的患者展示其首诊、首次TACE术中、首次TACE术后的影像资料(图6)。病灶特征相近情况下,在*B. dentium*丰度高组的患者,首次TACE术后碘油沉积良好,评估PR(图6A-D);在*B. dentium*丰度低组的患者,首次TACE术后碘油沉积较差,评估SD(图6E-H)。

## 3 讨论

### 3.1 整体菌群多样性并非动脉化疗栓塞联合靶免治疗疗效的敏感预测指标

本研究系统分析了接受TACE联合靶免治疗的中晚期HCC患者肠道菌群组特征,并探究了其临床预后的关联。我们的主要发现是:尽管患者整体肠道细菌、真菌群落的 $\alpha$ 与 $\beta$ 多样性在不同预后或治疗应答组间差异无统计学意义,但特定细菌及真菌物种的丰度与患者的PFS及对首次TACE的反应显著相关。这提示在TACE联合靶免治疗的

复杂背景下,肠道菌群对宿主预后的影响可能经由特定的“功能菌种”来实现。

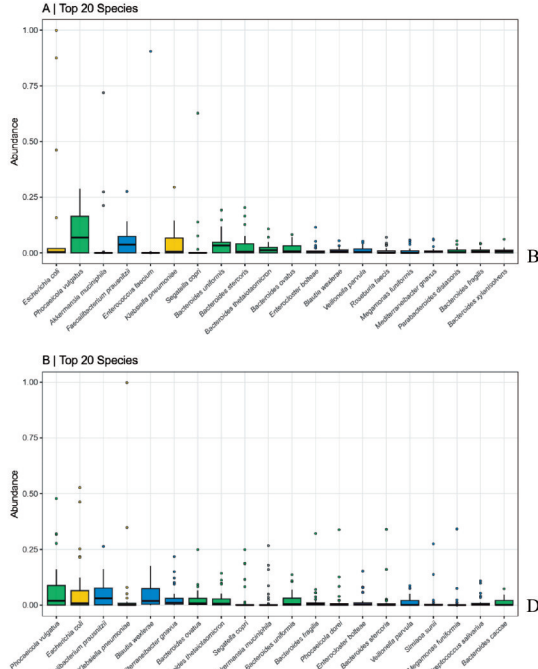
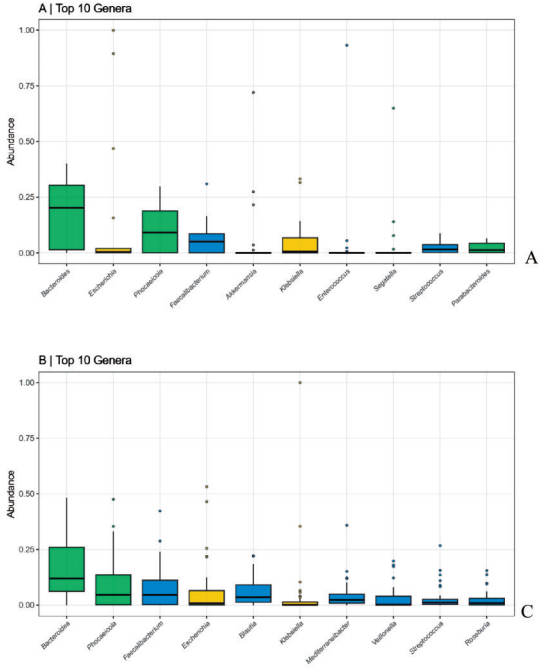
首先,本研究发现组间患者的年龄、性别、肿瘤负荷等基线特征差异无统计学意义,这有效排除了这些常见混杂因素对菌群-预后关联分析的干扰,增强了后续发现的可信度<sup>[24]</sup>。此外,无论预后或反应如何,拟杆菌属(*Bacteroides*)均在肠道菌群中占据主导地位,这与该菌属作为健康成人肠道核心共生菌的认知一致<sup>[25]</sup>。同时,普通拟杆菌(*Phocaeicola vulgatus*)和普拉梭菌(*Faecalibacterium prausnitzii*)在各组中均丰度较高,后者作为一种重要的产丁酸盐菌,其抗炎特性已被广泛报道,可能在维持基础肠道稳态中发挥作用<sup>[26]</sup>。然而,其普遍存在也意味着它可能并非区分治疗反应差异的关键标志物。

### 3.2 特定细菌与真菌物种的富集与良好预后及治疗应答显著相关

本研究的核心发现在于LEfSe分析揭示的差异菌种。细菌层面,*L. johnsonii*、*B. dentium*和*C. difficile*在预后好组与应答组中均显著富集。这一“重叠”现象强烈暗示,这些菌种可能通过共享的生物学机制,同时促进了对TACE的初始良好反应和更长的疾病无进展生存期。其中,*L. johnsonii*和*B. dentium*作为益生菌相关物种,其富集与良好预后相关具有合理的生物学解释。研究表明,*L. johnsonii*能够通过调节菌群稳态和强化黏膜屏障,显著减少肠道细菌易位及其诱导的全身炎症;其代谢产物还可激活肠道树突状细胞,进而增强全身抗肿瘤免疫应答<sup>[27]</sup>。此外,某些双歧杆菌也能够增强肠道屏障功能、调节局部及全身免疫,并可能通过代谢产物间接增强抗肿瘤免疫应答,从而对免疫检查点抑制剂起到增敏作用<sup>[28]</sup>。相较而言,*C. difficile*作为经典的机会性致病菌,通常与抗生素相关性腹泻密切相关,其在预后良好组中的显著富集初看似乎自相矛盾。然而,近年来的研究提示,*C. difficile*特定菌株或其在特定代谢状态下,可能在肿瘤微环境中扮演复杂乃至有益的免疫调节角色<sup>[29]</sup>。另一种可能是,该信号反映了更广泛的梭菌纲(*Clostridia*)成员的生态变化,这类细菌中包含许多产丁酸盐的菌种,与抗肿瘤免疫正相关<sup>[30]</sup>。我们的分析在属或种水平的分辨率可能不足以区分其具体的致病或共生亚型,这需要未来通过菌株水平测序或培养组学进一步验证。

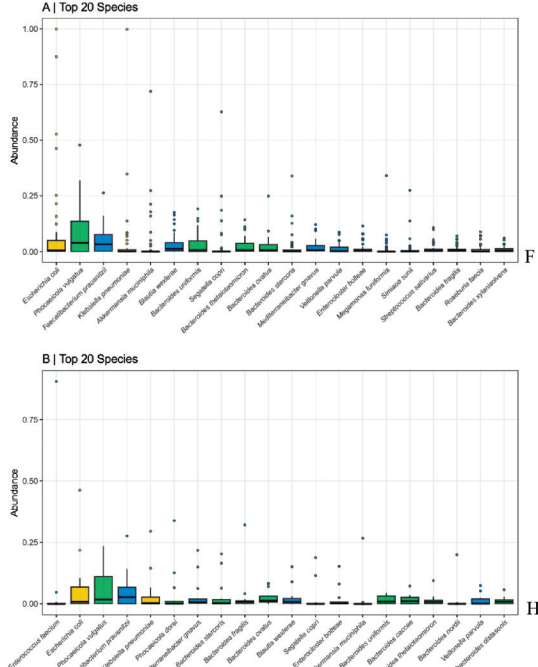
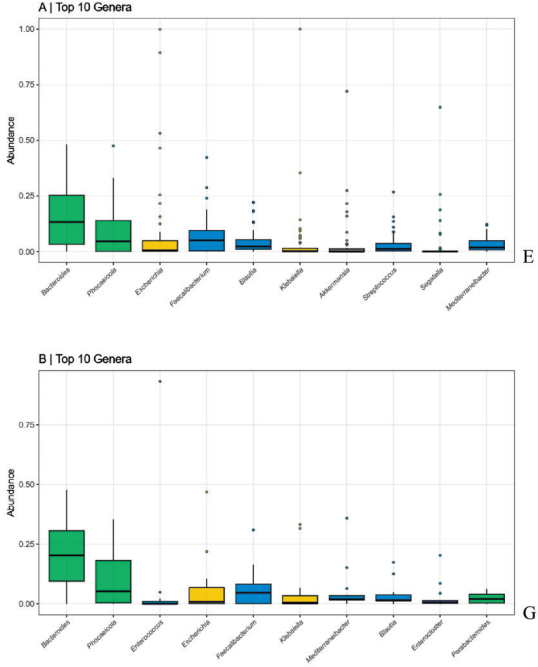
Composition Boxplot (Top taxa within each group)

Left: Genus Top10; Right: Species Top20; Groups: A (top) / B (bottom)



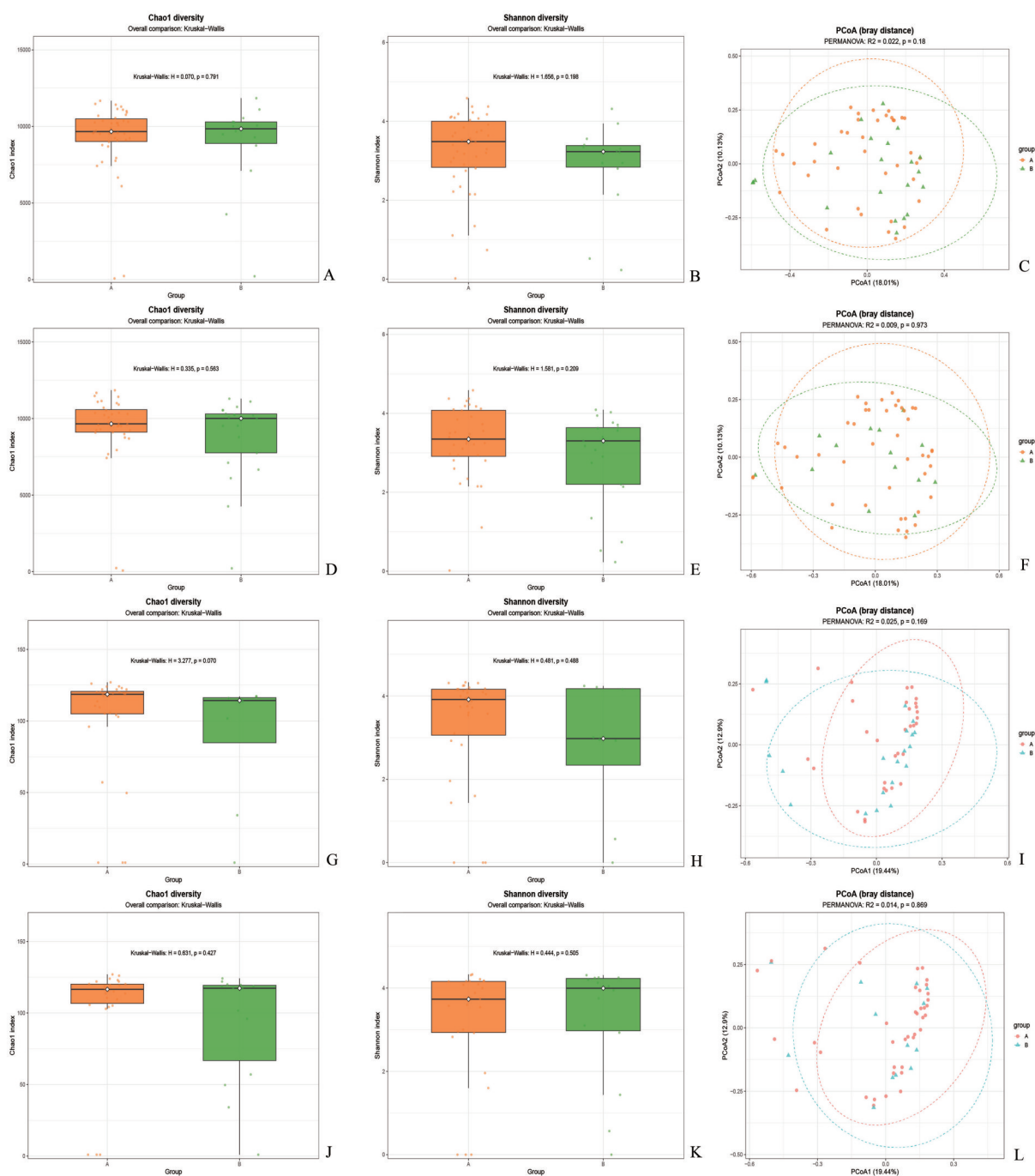
Composition Boxplot (Top taxa within each group)

Left: Genus Top10; Right: Species Top20; Groups: A (top) / B (bottom)



The top 10 bacterial relative abundances at the genus level for the good prognosis group, poor prognosis group, responding group, and non-responding group (A, C, E, G). The top 10 bacterial relative abundances at the species level for the good prognosis group, poor prognosis group, responding group, and non-responding group (B, D, F, H).

图 1 优势菌群  
Fig. 1 Dominant microbiota



The Chao1 index ( $H=0.070$ ,  $P=0.791$ ) and Shannon index ( $H=1.656$ ,  $P=0.198$ ) of bacterial  $\alpha$  diversity between groups grouped by prognosis (A–B). The Chao1 index ( $H=0.335$ ,  $P=0.563$ ) and Shannon index ( $H=1.581$ ,  $P=0.209$ ) of bacterial  $\alpha$  diversity between groups grouped by presence or absence of response after the first TACE (D–E). The results of principal coordinates analysis (PCoA) of bacterial  $\beta$  diversity between groups grouped by prognosis and by presence or absence of response after the first TACE (C, F). The Chao1 index ( $H=3.277$ ,  $P=0.070$ ) and Shannon index ( $H=0.481$ ,  $P=0.488$ ) of fungal  $\alpha$  diversity between groups grouped by prognosis (G–H). The Chao1 index ( $H=0.631$ ,  $P=0.427$ ) and Shannon index ( $H=0.444$ ,  $P=0.505$ ) of fungal  $\alpha$  diversity between groups grouped by presence or absence of response after the first TACE (J–K). The results of PCoA of fungal  $\beta$  diversity between groups grouped by prognosis and by presence or absence of response after the first TACE (I, L).

图2 组间多样性分析

Fig. 2 Inter-group diversity analysis



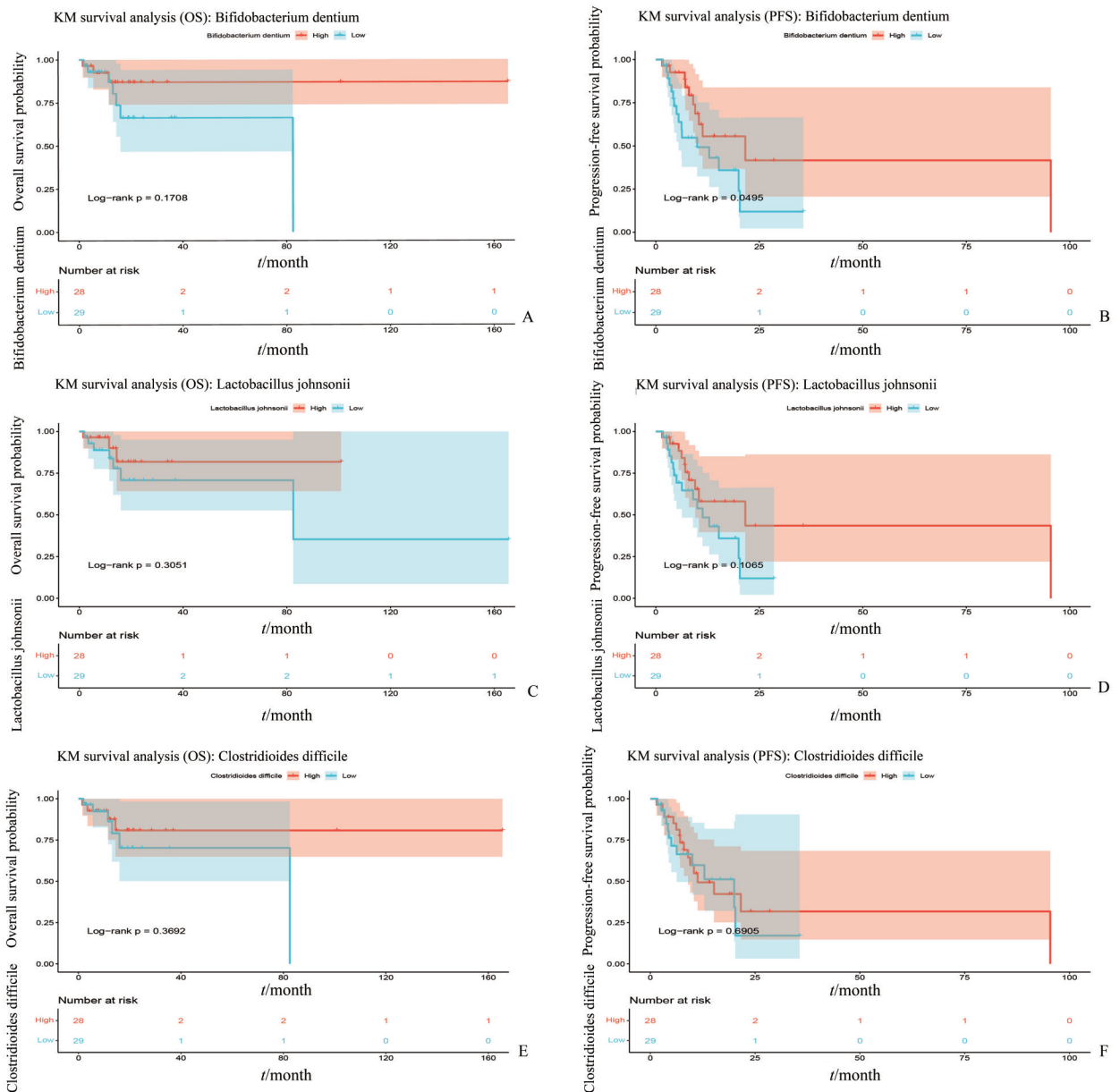
Based on the analysis at the genus level, the top 10 bacterial genera with significant differences between groups categorized by prognosis and by the presence or absence of response to the initial TACE treatment (A, B). At the species level, the top 10 bacterial species with significant differences between groups categorized by prognosis and by the presence or absence of response to the initial TACE treatment (C, D). The top 10 fungal species with significant differences between groups categorized by prognosis and by the presence or absence of response to the initial TACE treatment (E, F). Red indicates a higher relative abundance in Group A (good prognosis group/responding group), while blue indicates a higher relative abundance in Group B (poor prognosis group/non-responding group).

图3 组间菌群构成差异

Fig. 3 Differences in gut microbiota community composition between groups

真菌层面, *C. decagattii* 在预后良好组中富集 同样值得深入探讨。隐球菌属 (*Cryptococcus*) 真菌

通常被认知为机会性病原体, 但其与免疫系统的相互作用十分复杂。近年研究表明, 某些隐



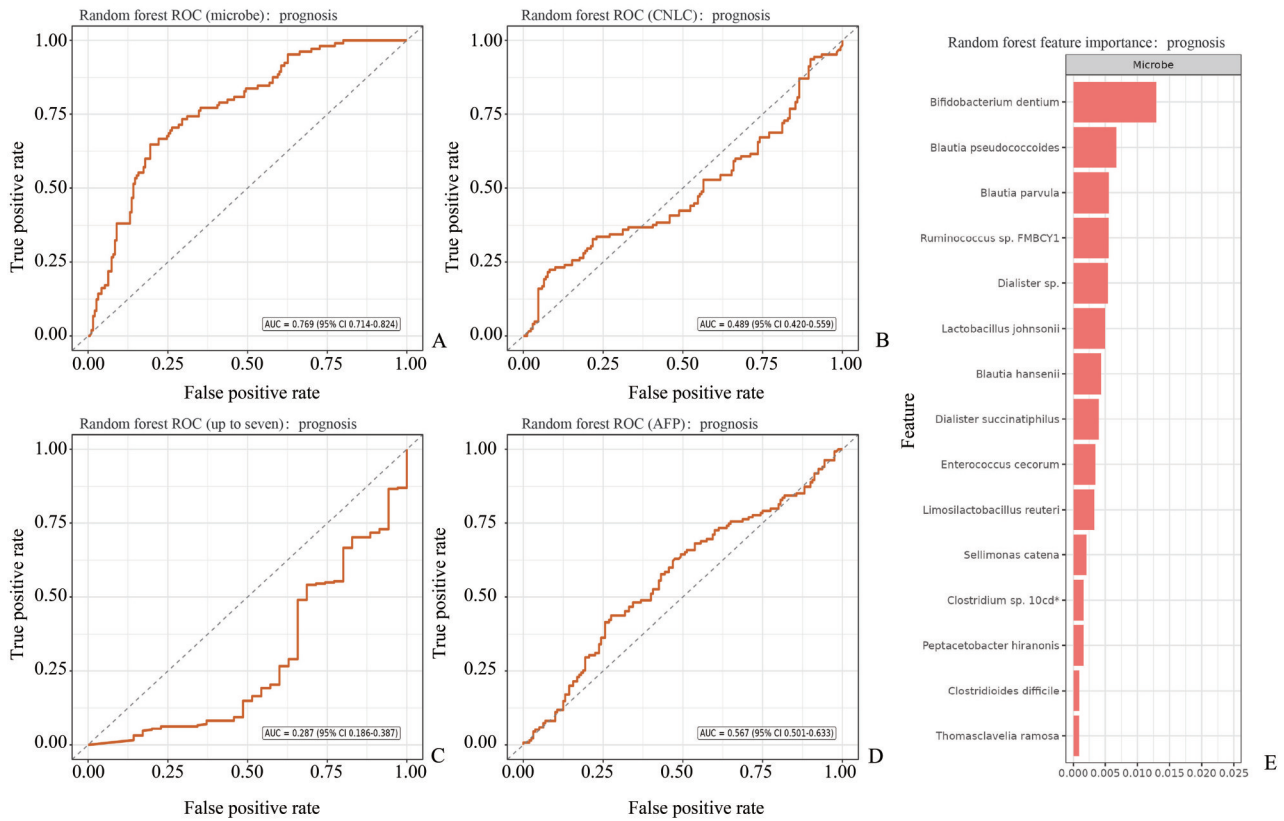
A comparison of OS differences between the two groups grouped by the median abundance of *B. dentium*, *L. johnsonii*, and *C. difficile* (A, C, E). A comparison of PFS differences between the two groups grouped by the median abundance of *B. dentium*, *L. johnsonii*, and *C. difficile* (B, E, F). Red indicates the high abundance group, and blue indicates the low abundance group.

图4 差异菌丰度分组的生存分析

Fig. 4 Survival analysis of differential bacterial abundance grouping

球菌物种或其细胞壁成分(如葡萄糖醛酸木糖甘露半乳聚糖,GXMGal)能够调节树突状细胞、巨噬细胞等固有免疫细胞的功能,并在特定情境下可能诱导具有抗肿瘤潜能的免疫应答<sup>[31]</sup>。因此,*C. decagattii*在好预后组中的富集,可能暗示其参与塑造了一种更有利于抗肿瘤免疫的肠道微环境。此外,*P. striiformis*与*K. dendrophila*作为环境或植物相关真菌在人体肠道中被检出,其来源与意义尚

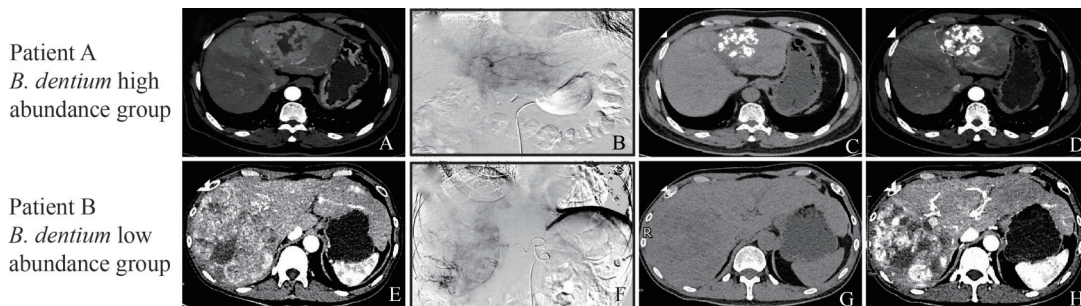
不明确,需谨慎解读其生物学意义;可能反映了饮食或环境暴露的差异,但与其与预后的关联提示它们或可作为潜在的菌群标志物<sup>[32]</sup>。在治疗反应层面,*K. bestiolae*在应答组中富集,其积极作用机制有待阐明,但与其与治疗反应的正相关性提示,特定的真菌构成可能有助于提升肿瘤对治疗的敏感性。



Receiver operating characteristic (ROC) curves for the prognostic prediction model constructed based on microbial characteristics, clinical stage, tumor burden, and AFP level (A-D). Random forest assessment of microbial model feature importance (E).

图5 不同预后预测模型的ROC曲线比较

Fig. 5 Comparison of ROC curves of different prognostic prediction models



The images above show patients with high abundance of *B. dentium* (A, B, C, D), while the images below show patients with low abundance of *B. dentium* (D, E, F, H). From left to right are the imaging images of the first visit, the first TACE surgery period, the first TACE postoperative plain scan, and the first TACE postoperative arterial phase.

图6 病历展示

Fig. 6 Representative medical record

### 3.3 齿双歧杆菌是潜在的预后生物标志物

生存分析提示根据 *B. dentium* 相对丰度高低分组的患者, PFS 差异具有统计学意义, 这直接证实了该菌种作为潜在预后生物标志物的价值。更具说服力的是, 通过机器学习构建的多种预后模型比较证实, 基于肠道菌群特征的预测模型效能优于

传统的临床分期(CNLC)、肿瘤负荷(up-to-seven)及血清AFP模型。且随机森林特征重要性分析将 *B. dentium* 明确识别为该菌群模型中的首要预测因子。这些数据强有力地支持以下观点: 粪便 *B. dentium* 丰度可能是一个潜在的、非侵入性生物标志物, 且在预测中晚期肝癌TACE联合靶免治疗预

后方面可能优于部分传统指标,为临床预后评估体系提供了新的菌群维度。

当然,本研究存在一定的局限性。首先,本研究为单中心回顾性研究且样本量( $n=61$ )相对较小,研究仅分析了治疗前的肠道菌群,缺乏对治疗过程中及治疗后肠道菌群的动态监测数据,因此无法确定关键菌群的变化轨迹及其对预后的因果性影响;未来需要前瞻性研究进行动态采样以验证和深化本研究的发现<sup>[33]</sup>。其次,本研究主要进行了相关性描述,尽管结合了生存分析,但肠道菌群影响疗效的具体分子机制(如代谢产物、免疫细胞表型变化)尚未阐明。此外,我们主要关注了治疗前的菌群特征,治疗过程中的动态演变及其对疗效的反馈影响未被监测<sup>[34]</sup>。

综上所述,本研究表明,在接受TACE联合靶免治疗的中晚期HCC患者中,肠道菌群的整体多样性可能并非预测预后的敏感指标,而以*L. johnsonii*、*B. dentium*等为代表的特定菌种,则显示出作为预测治疗反应和PFS的潜在菌群标志物的价值。尤其值得深入探究的是,*C. difficile*、*C. decagattii*等在此背景下所呈现的“正向关联”背后的生物学机制。未来研究应扩大队列,并整合宏基因组学、代谢组学及免疫图谱分析,以揭示这些标志性菌种影响疗效的具体机制。最终,通过膳食干预、益生菌/元或选择性菌群移植等手段调控肠道菌群,有望成为优化中晚期HCC联合治疗策略、实现个体精准化治疗的新途径。

#### 参考文献

- [1] Bray F, Laversanne M, Sung H, et al. Global cancer statistics 2022: GLOBOCAN estimates of incidence and mortality worldwide for 36 cancers in 185 countries [J]. CA Cancer J Clin, 2024, 74(3): 229-263.
- [2] 吴广东, 卢倩. 肝癌肝移植的全流程管理[J]. 器官移植, 2025, 16(2): 214-219.  
Wu GD, Lu Q. Full-process management of liver transplantation for hepatocellular carcinoma [J]. Organ Transp, 2025, 16(2): 214-219.
- [3] Llovet JM, De Baere T, Kulik L, et al. Locoregional therapies in the era of molecular and immune treatments for hepatocellular carcinoma [J]. Nat Rev Gastroenterol Hepatol, 2021, 18(5): 293-313.
- [4] Finn RS, Qin S, Ikeda M, et al. Atezolizumab plus bevacizumab in unresectable hepatocellular carcinoma [J]. N Engl J Med, 2020, 382(20): 1894-1905.
- [5] 赵紫薇, 崔玉秀, 刘惠敏, 等. 外周血异常凝血酶原、甲胎蛋白异质体-L3联合游离线粒体DNA对经导管动脉化疗栓塞术治疗原发性肝癌患者预后预测价值[J]. 临床军医杂志, 2026, 54(3): 304-307.  
Zhao ZW, Cui YX, Liu HM, et al. The prognostic value of peripheral blood abnormal prothrombin, alpha fetoprotein heterologo-L3 combined with free mitochondrial DNA in patients with primary liver cancer treated with transcatheter arterial chemoembolization [J]. Clin J Med Officers, 2026, 54(3): 304-307.
- [6] Kudo M. Combination cancer immunotherapy with molecular targeted agents/anti-PD-1 antibody for hepatocellular carcinoma [J]. Liver Cancer, 2019, 8(1): 1-11.
- [7] Yu LX, Schwabe RF. The gut microbiome and liver cancer: mechanisms and clinical translation [J]. Nat Rev Gastroenterol Hepatol, 2017, 14(9): 527-539.
- [8] Ponziani FR, Bhoori S, Castelli C, et al. Hepatocellular carcinoma is associated with gut microbiota profile and inflammation in independent of etiology [J]. Hepatology, 2019, 69(3): 1074-1088.
- [9] Tripathi A, Debelius J, Brenner DA, et al. The gut-liver axis and the intersection with the microbiome [J]. Nat Rev Gastroenterol Hepatol, 2018, 15(7): 397-411.
- [10] 孟志超, 周林, 刘毓玲, 等. 茯苓多糖对非酒精性脂肪肝相关肝细胞癌小鼠肠道菌群、肝功能的影响[J]. 联勤军事医学, 2025, 39(1): 11-15.  
Meng ZC, Zhou L, Liu YL, et al. Effects of poria cocos polysaccharide on intestinal flora and liver function of mice with nonalcoholic fatty liver associated hepatocellular carcinoma [J]. Mil Med Jnt Log, 2025, 39(1): 11-15.
- [11] Gopalakrishnan V, Spencer CN, Nezi L, et al. Gut microbiome modulates response to anti-PD-1 immunotherapy in melanoma patients [J]. Science, 2018, 359(6371): 97-103.
- [12] Routy B, Le Chatelier E, Derosa L, et al. Gut microbiome influences efficacy of PD-1-based immunotherapy against epithelial tumors [J]. Science, 2018, 359(6371): 91-97.
- [13] Zheng Y, Wang T, Tu X, et al. Gut microbiome affects the response to anti-PD-1 immunotherapy in patients with hepatocellular carcinoma [J]. J Immunother Cancer, 2019, 7(1): 193.
- [14] Bai L, Yan X, Qi P, et al. Effect of transarterial

- chemotherapy on the structure and function of gut microbiota in New Zealand white rabbits[J]. *Biology (Basel)*, 2024, 13(4): 230.
- [15] Li R, Liu J, Ye F, et al. Microbial metabolism dysfunction induced by transarterial chemoembolization aggravates postprocedural liver injury in HCC [J]. *J Hepatol*, 2025, S0168-8278(25)02557-7.
- [16] Bian CF, Wang Y, Yu A, et al. Gut microbiota changes and biological mechanism in hepatocellular carcinoma after transarterial chemoembolization treatment [J]. *Front Oncol*, 2022, 12: 1002589.
- [17] Yang J, Lim J, Kim EH, et al. Prognostic role of short-chain fatty acid-producing gut microbiota and gut microbial dynamics in patients with hepatocellular carcinoma receiving chemoembolization: a prospective study [J]. *J Hepatocell Carcinoma*, 2025, 12: 1991-2004.
- [18] Mao J, Wang D, Long J, et al. Gut microbiome is associated with the clinical response to anti-PD-1 based immunotherapy in hepatobiliary cancers [J]. *J Immunother Cancer*, 2021, 9(12): e003334.
- [19] Inukai Y, Yamamoto K, Honda T, et al. Intestinal microbiome associated with efficacy of atezolizumab and bevacizumab therapy for hepatocellular carcinoma [J]. *Cancers (Basel)*, 2024, 16(9): 1675.
- [20] Lee PC, Wu CJ, Hung YW, et al. Gut microbiota and metabolites associate with outcomes of immune checkpoint inhibitor-treated unresectable hepatocellular carcinoma [J]. *J Immunother Cancer*, 2022, 10(6): e004779.
- [21] Liu C, Wang Z, Zhang H, et al. Gut microbiota modulates tumor metastasis through the hepatic portal vein [J]. *Cell Rep*, 2021, 36(11): 109703.
- [22] 中华人民共和国国家卫生健康委员会医政司. 原发性肝癌诊疗指南(2024年版)[J]. *协和医学杂志*, 2024, 15(3): 532-559.  
Department of Medical Administration, National Health Commission of the People's Republic of China. Guidelines for the diagnosis and treatment of primary liver cancer (2024 Edition) [J]. *Med J Pumch*, 2024, 15(3): 532-559.
- [23] Lencioni R, Llovet JM. Modified RECIST (mRECIST) assessment for hepatocellular carcinoma [J]. *Semin Liver Dis*, 2010, 30(1): 52-60.
- [24] Wong GLH, Wong VWS, Tan GM, et al. Surveillance programme for hepatocellular carcinoma improves survival in high-risk patients: a prospective study [J]. *Liver Int*, 2019, 39(7): 1314-1324.
- [25] Wexler AG, Goodman AL. An insider's perspective: Bacteroides as a window into the microbiome [J]. *Nat Rev Microbiol*, 2017, 15(4): 207-220.
- [26] Miquel S, Martin R, Rossi O, et al. Faecalibacterium prausnitzii and human intestinal health [J]. *Curr Opin Microbiol*, 2013, 16(3): 255-261.
- [27] Jia D, Wang Q, Qi Y, et al. Microbial metabolite enhances immunotherapy efficacy by modulating T cell stemness in pan-cancer [J]. *Cell*, 2024, 187(7): 1651-1665.e21.
- [28] Sivan A, Corrales L, Hubert N, et al. Commensal Bifidobacterium promotes antitumor immunity and facilitates anti-PD-L1 efficacy [J]. *Science*, 2015, 350(6264): 1084-1089.
- [29] Pushalkar S, Hundeyin M, Daley D, et al. The pancreatic cancer microbiome promotes oncogenesis by induction of innate and adaptive immune suppression [J]. *Cancer Discov*, 2018, 8(4): 403-416.
- [30] Jani CT, Edwards K, Bhanushali C, et al. Leveraging beneficial microbiome-immune interactions via probiotic use in cancer immunotherapy [J]. *Front Immunol*, 2025, 16: 1713382.
- [31] Guimarães-de-Oliveira JC, da Silva-Junior EB, Meyrelles MSM, et al. Immunomodulatory effects of *Cryptococcus neoformans* capsular polysaccharides on macrophage infected with *Trypanosoma cruzi* [J]. *Acta Trop*, 2025, 271: 107849.
- [32] Nash AK, Auchtung TA, Wong MC, et al. The gut mycobiome of the human microbiome project healthy cohort [J]. *Microbiome*, 2017, 5(1): 153.
- [33] Ma C, Han M, Heinrich B, et al. Gut microbiome-mediated bile acid metabolism regulates liver cancer via NKT cells [J]. *Science*, 2018, 360(6391): eaan5931.
- [34] Derosa L, Routy B, Thomas AM, et al. Intestinal *akkermansia muciniphila* predicts clinical response to PD-1 blockade in patients with advanced non-small-cell lung cancer [J]. *Nat Med*, 2022, 28(2): 315-324.

(编辑 余菁)